Effect of Nozzle Port Angle on Mold Surface Flow in Steel Slab Casting

Seong-Mook Cho[1], Brian G. Thomas[1,2], Hyoung-Jun Lee[3], Seon-Hyo Kim[3]

[1]University of Illinois at Urbana-Champaign
Department of Mechanical Science and Engineering
1206 West Green Street, Urbana, IL 61801, USA
Phone: 217-333-6919
E-mail: y104401@illinois.edu

[2]Colorado School of Mines
Department of Mechanical Engineering
1500 Illinois Street, Golden, Colorado 80401, USA
Phone: 303-273-3309
E-mail: bgthomas@mines.edu, bgthomas@illinois.edu

[3]Pohang University of Science and Technology
Department of Materials Science and Engineering,
San31, Hyoja-Dong, Nam-Gu, Pohang, Kyungbuk 790-784, Republic of Korea
Phone: 82-54-279-5968

Keywords: continuous casting, surface instability, jet flow, standard k-tabilit, water model

ABSTRACT

Nozzle port angle is a critical parameter controlling fluid flow in the continuous casting mold, especially across the top surface. Fluid flow calculations with a three-dimensional (3-D) k-D model and die-injection experiments on a 1/3 scale water model were performed to quantify the effects of nozzle angle on flow pattern and surface flow. Calculated results are compared with surface velocity measurements with an electromagnetic sensor. The 15° up-angled nozzle produces more severe jet wobbling for the conditions simulated, resulting in lower velocity and higher velocity fluctuations at the surface. This could increase surface cracks, powder entrapment, and associated downstream problems, especially in advanced high-strength steels.

INTRODUCTION

During the continuous casting of steel slabs, abnormal surface velocity, surface level, and their fluctuations are major causes of surface quality problems in final rolled products. Surface level fluctuations near the solidifying steel shell on the Narrow Faces (NF) and Wide Faces (WF), can entrap surface mold flux into the solidifying steel shell [1-3]. Excessive surface velocity increases shear instability at the liquid mold flux/molten steel interface, resulting in mold flux entrainment [4-6]. On the other hand, surface velocity that is too slow can produce low and non-uniform surface temperature, including meniscus freezing, hook formation [7,8], and surface defects related to initial solidification problems.

To control surface velocity and level, many efforts have been made to optimize nozzle port design, and casting conditions, including gas-injection and electromagnetic systems. Nozzle design is one of the most important process parameters that can be easily changed in the steel plant, to optimize the surface velocity. Lee et. al. investigated the effect of nozzle bottom shapes (well- and mountain-type bottom) on surface velocity and its fluctuations [9]. They found that the mountain-type bottom produces higher velocity and more unstable flow and turbulence at the top surface, causing higher variations in the surface-level profile, level fluctuations, and easier slag entrainment, owing to its increased sensitivity to flow variations; thus the

well-bottom nozzle is better for steel quality. Najjar et. al. investigated the effect of nozzle design (port angle, port dimensions (height, width, thickness), port side dispersion angle, port shape, bottom design, number of ports) on nozzle flow [10]. They found that deeper (more-downward) angled nozzle-ports produce deeper jet angle. This work applies both 1/3 scale water model experiments and computational modeling of the water model to investigate the effect of nozzle port angle on not only nozzle flow, but also mold flow pattern, surface velocity, and turbulence, for a different set of casting conditions.

METHODOLOGY

Water Model Experiment

A one-third scale water model of the real continuous caster, shown in Figure 1, was used for experiments to measure nozzle and mold flow. The water model consists of a half tundish, stopper-rod, Submerged Entry Nozzle (SEN), and mold. The water flow rate from the tundish through the SEN into the mold is controlled by changing the size of the annular gap between the stopper and the bottom of the tundish. Water at 25°C exits holes in the mold bottom to a holding water bath and is pumped continuously back up to the tundish. Two different nozzle ports shown in Figure 2 were investigated in this study of the effect of port angle on the mold surface flow. Both nozzles were bifurcated with typical rectangular ports with slightly rounded corners, differing only regarding the angle of the ports: +15f (up-angle) or -15p (down-angle) at both upper and lower edges. Table 1 provides details of the casting conditions, nozzle and mold dimensions of the real caster and the 1/3 scale water model. The casting speed was chosen based on maintaining a constant Froude number, which is defined as the ratio of inertia force to gravitational force as follows

$$\left(V_{Casting,W}/\sqrt{gL_W}\right) = \left(V_{Casting,R}/\sqrt{gL_R}\right) \quad (1)$$

where W is for water model, R is real caster, $V_{casting}$ is casting speed, L is scale length, and g is gravitational acceleration.

Rearranging this equation gives the casting speed in the water model, $V_{Casting,\,W}$ as follows:

$$V_{Casting,W} = V_{Casting,R}\sqrt{L_W/L_R} \quad (2)$$

Measurements of instantaneous surface velocity were performed using an electromagnetic current sensor located at the three positions shown in Figure 3: 1) 30mm from Narrow Face (NF), 2) W/8, W/4 positions on the left NF, 3) 10mm from free surface in the water model (W: mold width). Instantaneous horizontal velocity data was collected for 1000 sec at 10 Hz. The sensor can measure two components of horizontal surface velocity: one parallel and the other perpendicular to the mold width direction. In addition, dye and a small amount (0.06 % volume fraction of total volume flow rate of water and argon gas) of argon gas were injected to visualize the flow patterns. The visualized flow patterns were recorded with three video cameras to provide a NF end view, surface bottom view, and Wide Face (WF) front view.

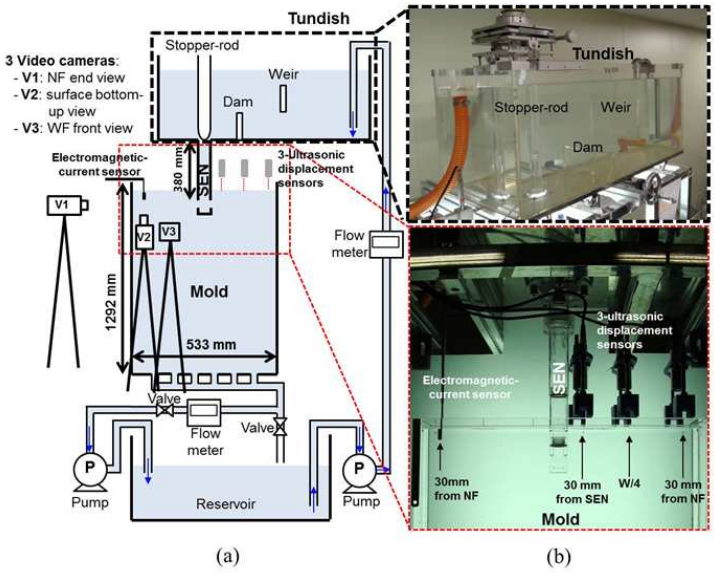

Figure 1. (a) Schematic and (b) photos of 1/3 scale water model

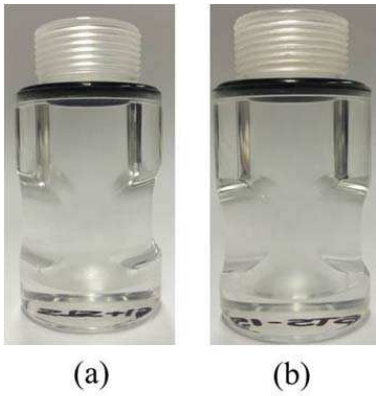

Figure 2. Nozzle ports: (a) +15ur(up-angle) and (b) -15e)(down-angle)

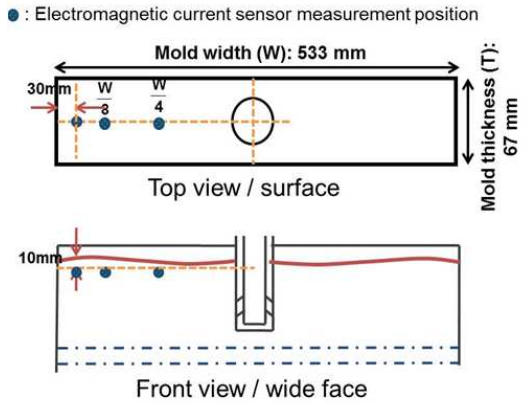

Figure 3. Sensor positions for measurements

Table 1. Caster dimensions and process conditions

	Real caster (R)	1/3 scale water model (W)
Casting speed	$V_{Casting, R}$: 0.8 m/min	$V_{Casting, W}$: 0.5 m/min
Volume Flow rate	256.0 LPM	16.4 LPM
Submerged depth of nozzle	140 mm	46.7 mm
Mold width	1600 mm	533 mm
Mold thickness	200 mm	67 mm
Aspect ratio between mold width and thickness	8.0	
Nozzle port angle	+15° (up-angle), -15° (down-angle)	
Nozzle port size (width x height / radius of rounded corner)	60 mm x 65 mm / 20 mm	20 mm x 21.7 mm / 6.7 mm
Nozzle bore (inner / outer)	Φ60 ~ 65 mm (from bottom to top) / Φ110 mm	Φ20.8 mm (average) / Φ36.6 mm
Area ratio between two ports and nozzle bore	2.54	
Ar gas injection	No gas	10 ml/min (0.06 % volume fraction for clear visualization of mold flows

Computational Modeling

To quantify the flow pattern in the nozzle and mold with the +15 l(up-angle) and -15ng(down- angle) nozzle port cases, a three-dimensional (3-D) finite-volume computational model was applied. The steady, incompressible, Reynolds Averaged Navier-Stokes (RANS) equations with the standard k - agmodel have been solved with the commercial computational fluid dynamics (CFD) package program, ANSYS FLUENT to estimate the time-averaged turbulent flow in the nozzle and mold.

The model used a one-quarter domain (adopting 4-fold symmetry) and included the tundish bottom region, nozzle and mold, as shown in Figure 4. The nozzle port in the domain was simplified to a rectangular shape, without the rounded corner. The SEN domain was connected with the mold domain and calculated together to obtain more accurate simulations of fluid flow in the mold [11]. Each case used a structured mesh of ~150,000 hexahedral cells. Constant velocity (0.000573 m/sec) was fixed as the inlet condition at the sides of the cylinder representing part of the tundish bottom, along with 10^{-5} m^2 /sec^2 for turbulent kinetic energy and 10^{-5} m^2 /sec^3 for turbulent dissipation rate. The velocity was calculated according to the flow rate in the water model and the surface area of the cylindrical sides of the tundish bottom region. At the mold bottom, outlet boundary conditions of 0 Pa of gauge pressure, 10^{-5} m^2/sec^2 for turbulent kinetic energy and 10^{-5} m^2 /sec^3 for dissipation rate were applied. The top surface of the mold was given by a stationary wall with 0 Pa shear stress components for free-slip boundary condition. For the two cases, convergence of solving the equations was defined when all scaled residuals were stably reduced below 10^{-4}.

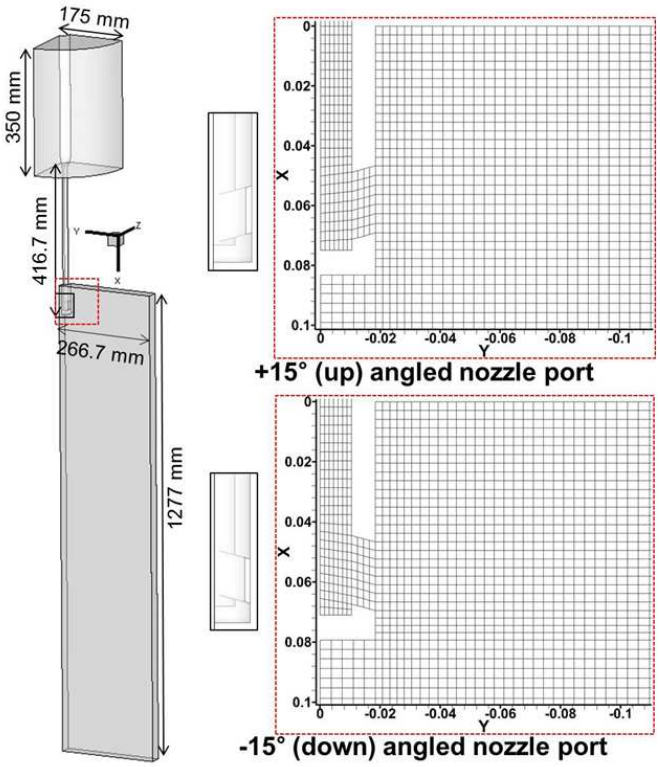

Figure 4. Domain and mesh

NOZZLE FLOW

To investigate the effect of nozzle port angle on nozzle flow pattern, velocity vectors with their magnitude contours are presented in Figure 5 for the +15re(up-angle) and -15de(down-angle) port cases. Jet flow into the mold is deeper with the -15 ° (downward-angled) port: the vertical jet angle in the casting direction is -19.3° with the -15° port and +1.12° with the +15 ° (up-angle) port. At the nozzle port exit, the jet flow with +15th(upward-angled) shows a larger flow-rotation region of swirl near the corner of the port sides.

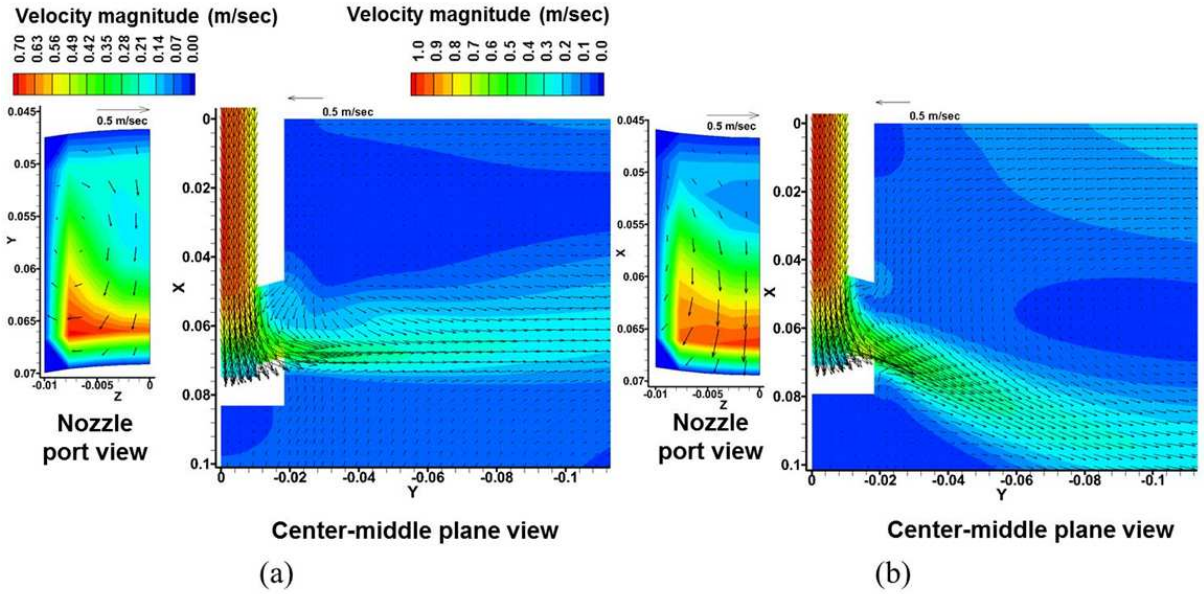

Figure 5. Nozzle flow patterns with (a) +15oz(up-angle) and (b) -15 p(down-angle) nozzle port

For more detailed analysis of swirl with different nozzle port angles, vorticity components in each axis and turbulent kinetic energy of nozzle flow are given in Figure 6. Vorticity vector, the curl of the velocity vector, describes the rotation of flow and is defined as follows:

$$\overrightarrow{\omega_i} = \nabla \times \overrightarrow{V_i} \tag{3}$$

where $\overrightarrow{\omega_i}$ is vorticity, ∇ is gradient, and $\overrightarrow{V_i}$ is velocity in the 3 coordinate directions (x, y, and z).

The +15e (up-angle) port produces higher vorticity components than the -15ha(down-angle) port does, especially y-vorticity. This produces higher vorticity magnitude and higher turbulent kinetic energy. The swirl rotation about the y-axis through the nozzle port contributes greatly to the flow fluctuations, resulting in ~2 times higher weighted-average turbulent kinetic energy: 0.0197 m^2/s^2 with the +15th(up-angle) port and 0.0101 m^2/s^2 with the -15th(down-angle) port. The predicted nozzle swirl phenomena are match well with those observed in the water model experiments, as shown in Figure 7. The measured swirl fills the entire port and alternates between clockwise and counter-clockwise directions. Due to the quarter domain of the current computational model, the predicted swirl region area was smaller than the measured one. A transient model with no symmetry assumption would be needed for realistic capture of the transient swirl behavior in the nozzle.

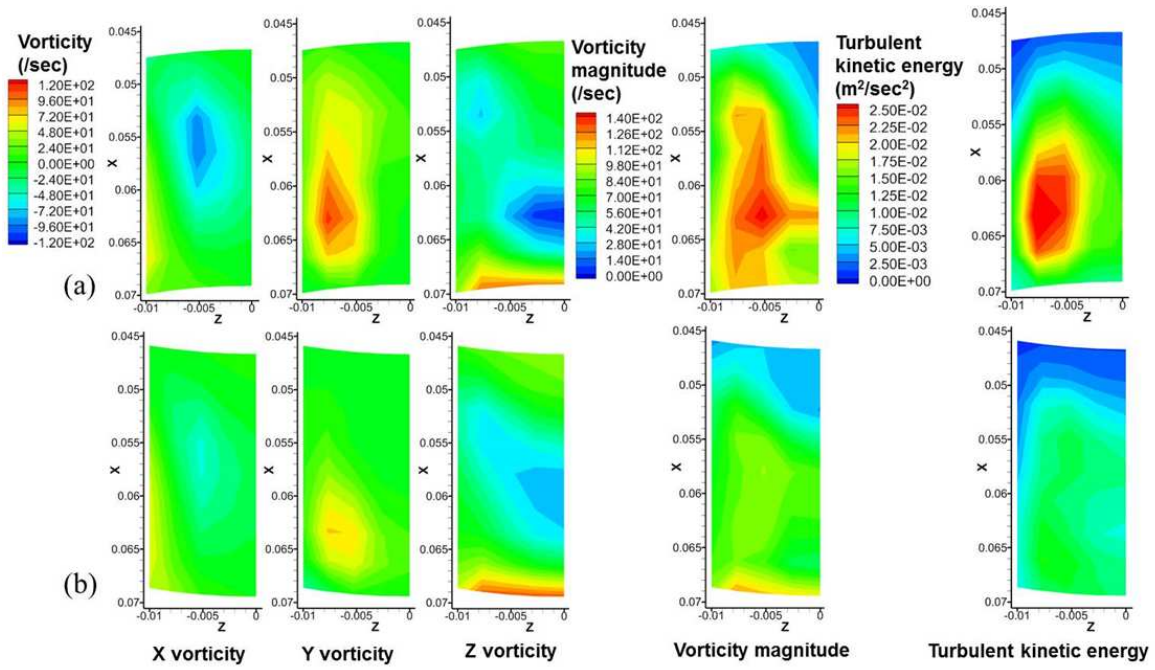

Figure 6. Time-averaged vorticity components and turbulent kinetic energy at nozzle port exit with (a) +15a)(up-angle) and (b) -15et(down-angle)

(a) (b)

Figure 7. Transient swirl at nozzle port exit with +15it(up-angle) in the 1/3 scale water model: (a) clockwise pattern and (b) counter-clockwise pattern

Further flow characteristics in the nozzle port exit are quantified with weighted-average calculations [12], and given in Table 2. As expected, decreasing nozzle port angle from +15r(up-angle) to -151(down-angle), produces higher downward velocity with deeper vertical jet angle (directed more steeply downwards). The horizontal jet angle becomes larger (directed more outward), and more towards the WF with higher outward velocity with the +15° (up-angle) port. In addition, the increased nozzle swirl with the +15t (up-angle) port causes: higher weighted average y vorticity, higher vorticity magnitude, and higher turbulent kinetic energy. The size of the backflow region remains almost the same.

Table 2. Jet characteristics

	+15° (up-angle)	-15° (down-angle)
Weighted-average x velocity (downward) (m/sec)	-0.011	0.176
Weighted-average y velocity (horizontal) (m/sec)	-0.565	-0.503
Weighted-average z velocity (outward) (m/sec)	-0.112	-0.0638
Vertical jet angle (degree)	+1.12 (towards surface)	-19.3 (towards mold exit)
Horizontal jet angle (degree)	-11.2	-7.23
Average jet speed (m/sec)	0.576	0.537
Maximum velocity magnitude (m/sec)	0.838	0.711
Weighted-average x vorticity (/sec)	-7.41	-1.18
Weighted-average y vorticity (/sec)	43.0	27.1
Weighted-average z vorticity (/sec)	-5.57	-20.8
Weighted-average vorticity magnitude (/sec)	108	72.1
Weighted-average turbulent kinetic energy(m^2/s^2)	0.0197	0.0101
Weighted-average turbulent kinetic energy dissipation rate (m^2/s^3)	0.669	0.269
Back-flow zone (%)	28.2	27.9

MOLD FLOW PATTERNS

Mold flow patterns predicted by the computational model for the two cases with different port angle are compared with those measured by dye injection in the 1/3 scale water model in Figure 8. The results using these two methods agree reasonably well. The +15e (up-angle) port produces a shallower jet angle. On the other hand, jet flow becomes deeper and more stable with the -15he(down-angle) port.

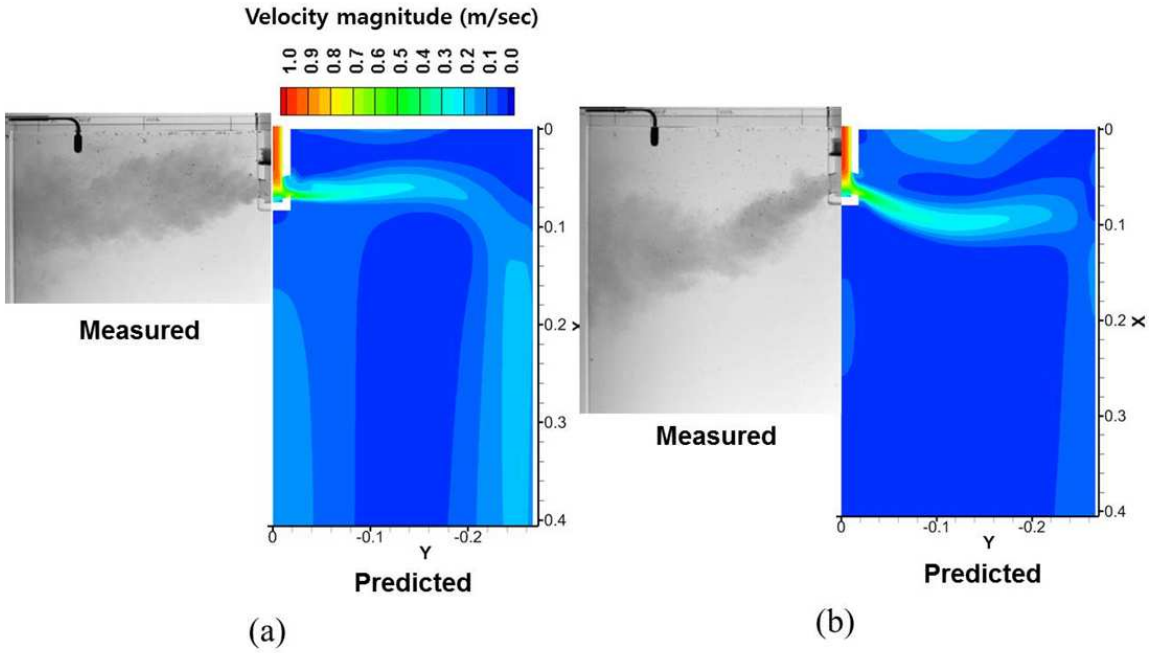

Figure 8. Mold flow patterns with (a) +15ol(up-angle) and (b) -15pa(down-angle) nozzle port

By comparing the dye diffusion areas in the visualized mold flow, jet wobbling phenomena were quantified and found to be more severe with the +15o (up-angle) port. As shown in Figure 9, this is due to the higher turbulent kinetic energy produced in the nozzle bottom, nozzle port, and upper region of the mold with this +15i (up-angle) port.

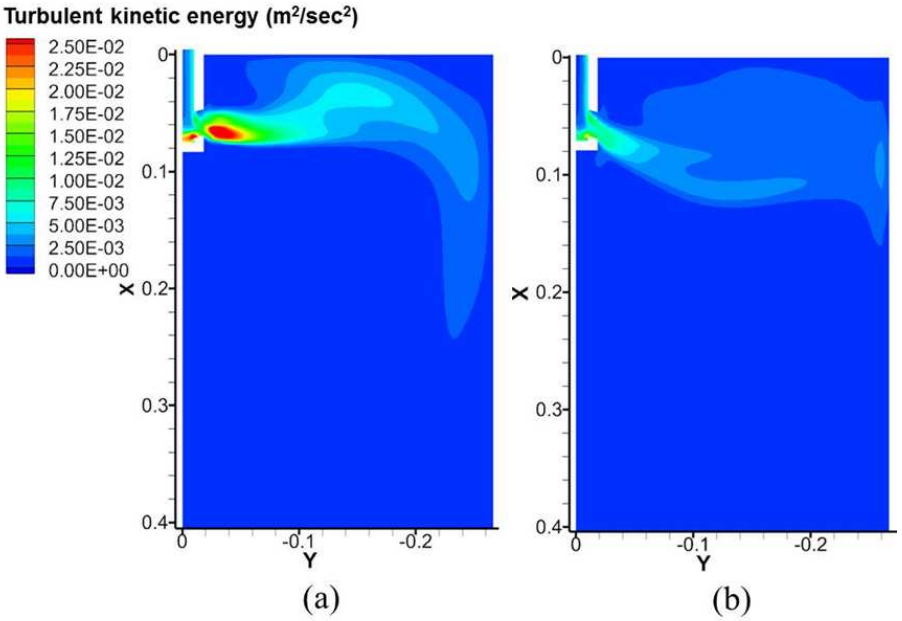

Figure 9. Turbulent kinetic energy of mold flow with (a) +15ur(up-angle) and (b) -15ki(down-angle) nozzle port

Vertical velocity of the jet flow in the casting direction down the NF increases with increasing (more upwards) jet angle, as shown in Figure 10. Because the jet flow from the +15° (up-angle) nozzle port impinges on the Inside Radius (IR) before reaching the NF as shown in Figure 11, the jet flow loses its upward momentum and bends to flow more downwards into the strand. One the other hand, the -15 e(down-angle) nozzle port produces a straighter jet flow directed towards the NF. The impingement angle on the NF is higher. Therefore, a higher momentum flow goes up the NF towards the surface, resulting higher surface velocity, as shown in Figure 12 b). However, surface velocity fluctuations are more severe with +15° (up-angle) nozzle due to larger jet flow wobbling, as indicated by the higher turbulent kinetic energy in Figure 12.

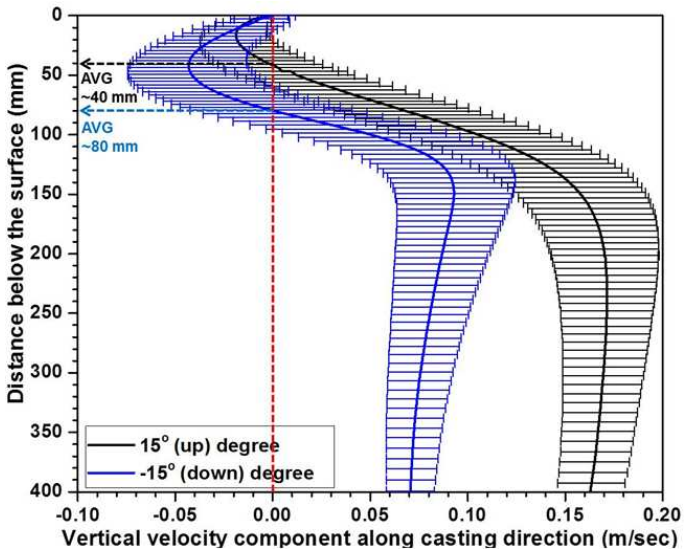

Figure 10. Vertical velocity near narrow face, along casting direction

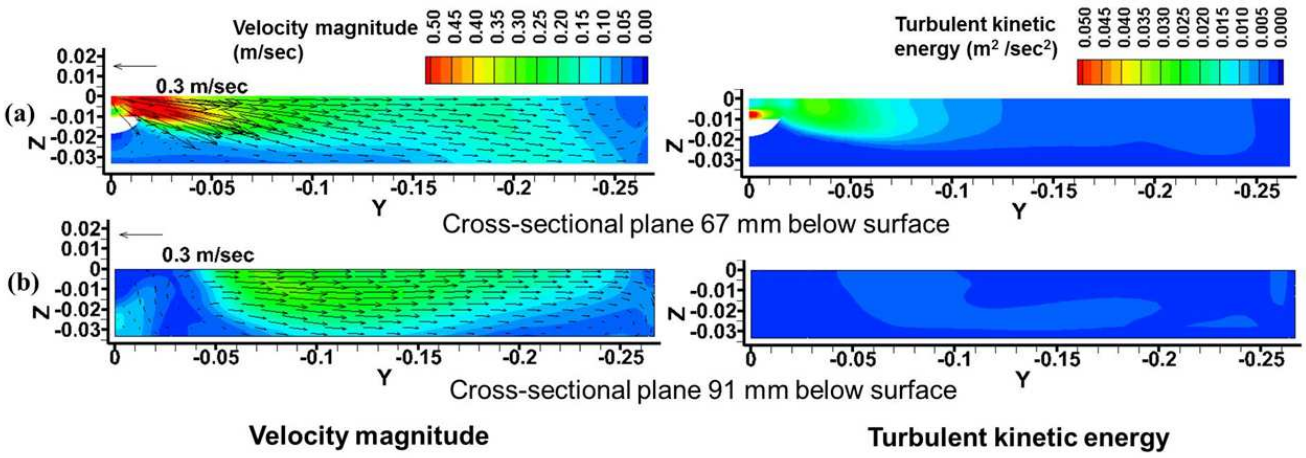

Figure 11. Jet patterns at cross-sectional plane with (a) +15it(up-angle) and (b) -15ec(down-angle) nozzle port

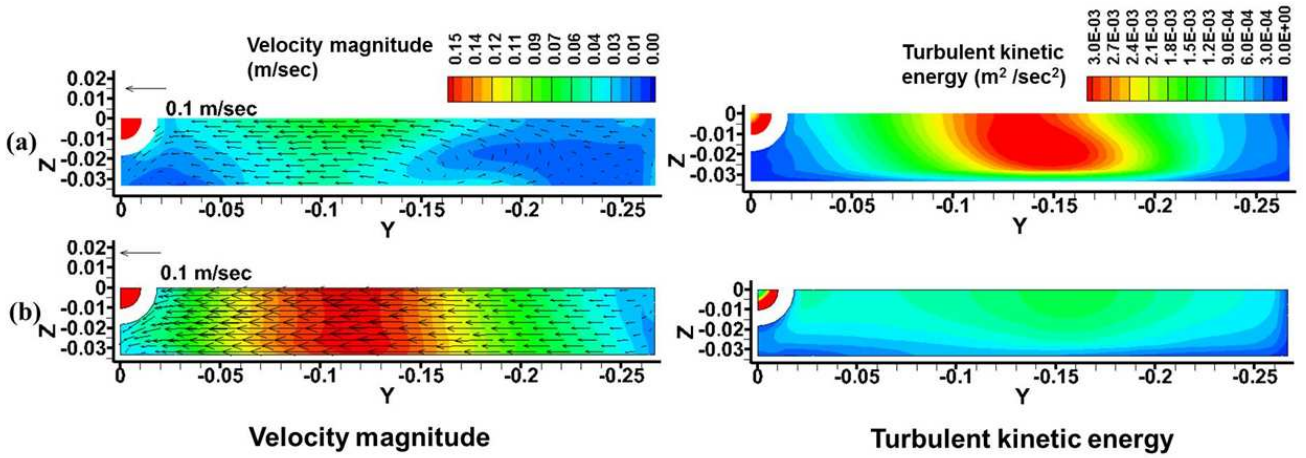

Figure 12. Flow patterns at cross-sectional plane 10mm below surface with (a) +15mm(up-angle) and (b) -15su(down-angle) nozzle port

TRANSIENT SURFACE FLOW VELOCITY

For more detailed investigation of the influence of nozzle port angle on surface velocity, instantaneous surface velocities were measured using the electromagnetic current sensor. Two-components of transient horizontal velocity (V_z: from inside radius to outside radius, V_y: from NF to SEN) were measured at three locations 10mm below the surface during 1000 sec, for both cases and are presented in Figure 13. The average and standard deviation of each velocity component is given in Table 3.

Horizontal velocity towards the SEN is higher than the other velocity component towards OR, at all three locations for both cases. Thus, the flow is generally towards the SEN, as expected from the results of the predicted mold flow patterns. Surface flow becomes faster towards the SEN with both +15EN(up-angle) and -15 l(down-angle) nozzle ports. Decreasing the nozzle port angle from +15z (up-angle) to -15p (down-angle) makes the surface flow from the NF to the SEN faster and more stable. Surface flow with +15fa(up-angle) nozzle port is slower and less stable, showing larger fluctuations, especially near the SEN.

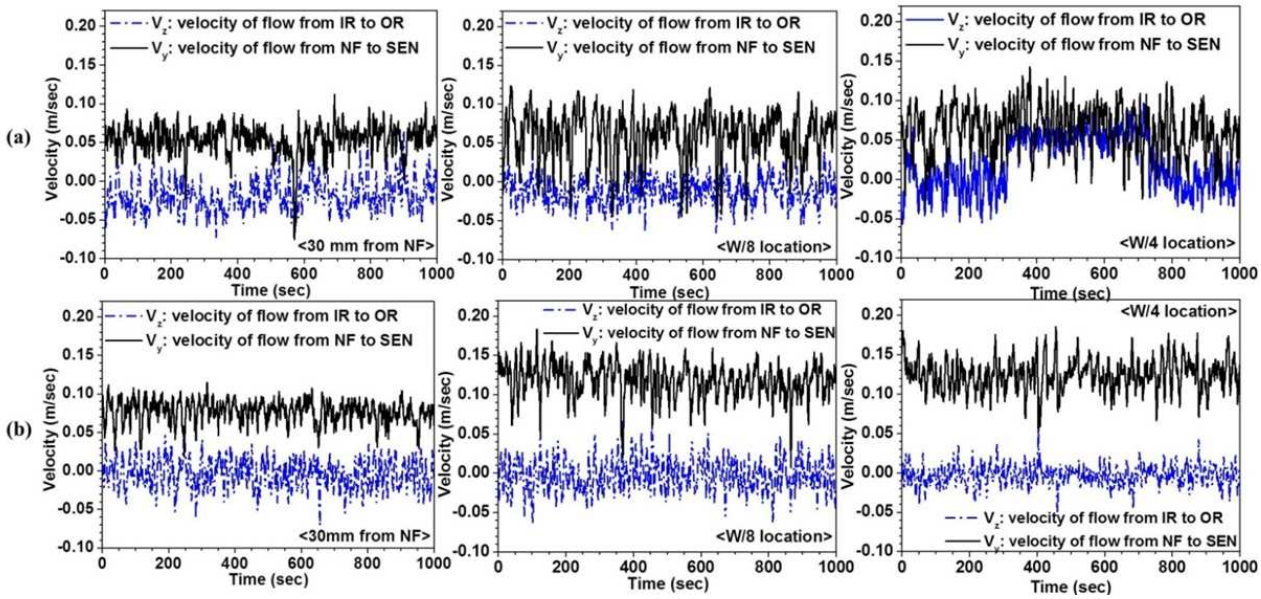

Figure 13. Measured instantaneous surface velocity histories at the three different surface positions across the mold width with (a) +15) (up-angle) and (b) -15ec(down-angle) nozzle port

Table 3. Measured time-averaged velocity and velocity fluctuations

		30 mm from NF	W/8 location	W/4 location
+15° (up-angle)	Velocity from NF to SEN	0.0535 ± 0.0189 m/sec	0.0595 ± 0.0310 m/sec	0.0628 ± 0.0292 m/sec
	Velocity from IR to OR	-0.0175 ± 0.0215 m/sec	-0.0118 ± 0.0173 m/sec	0.0218 ± 0.0335 m/sec
-15° (down-angle)	Velocity from NF to SEN	0.0768 ± 0.0144 m/sec	0.118 ± 0.0213 m/sec	0.124 ± 0.0199 m/sec
	Velocity from IR to OR	-0.00381 ± 0.0190 m/sec	-0.00266 ± 0.0204 m/sec	-0.00278 ± 0.0126 m/sec

Average surface velocities towards the SEN, in the centerplane, predicted by the RANS model, show good agreement with the measurements for both the +15eo(up-angle) and -15gl(down-angle) nozzle port cases. Although the trends are correct, the model over-predicts the measured velocity fluctuations, likely due to the assumption of isotropic turbulence of the k-ε model, which is insufficient to capture the real anisotropic fluctuations. Transient models, such as Large Eddy Simulation (LES), which can calculate more reasonable velocity fluctuations caused by anisotropic turbulence, are needed to improve the prediction of transient flow behavior, which is so important at the surface.

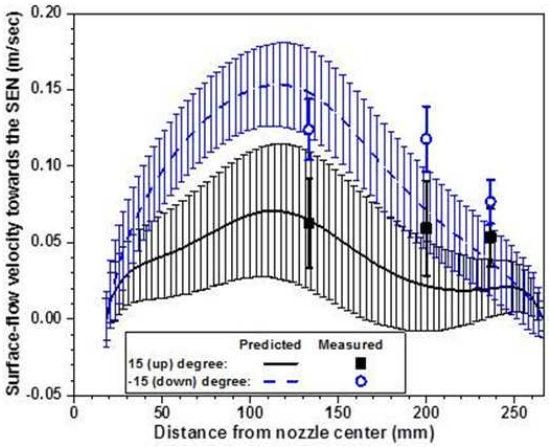

Figure 14. Comparison of surface velocity towards the SEN between the measurements and the computational predictions

SUMMARY AND CONCLUSIONS

Velocity measurements, die injection observations, and computational modeling with a standard k-o RANS model were applied to investigate the effect of nozzle port angle on time-averaged flow and flow variations in a 1/3-scale water model of the lower tundish, nozzle and mold during steady continuous slab casting of steel. Specifically, the effect of +15° (up-angle) and -15° (down-angle) nozzle port were investigated in a typical bifurcated port SEN submerged 140 mm in a 200 mm (thickness) x 1600mm (width) strand casting at 0.8 m/min.

- The RANS model prediction shows a very good quantitative match with mold flow patterns, average surface velocity profile, and surface velocity fluctuations measured in the 1/3 scale water model.
- Higher average surface velocity is produced with a port angle of -15elocity . Shallower port angle, +15wer po has slower surface velocity. Thus, in general, increased surface velocity occurs when the jet impinges first on the NF at an upward angle. That means that surface velocity is slower if the jet impinges first on the WF or near the corner.
- Jet flow from the +15° (up) nozzle port produces stronger swirl with higher vorticity and turbulent kinetic energy, resulting in more severe wobbling in the mold, than with -15th(down) ports; this up-angled jet sometimes impinges first on the top surface causing higher surface instability (low-frequency high-amplitude fluctuations), even though it has lower surface velocity, for these casting conditions.
- Unstable flow pattern results from the +15l (up) nozzle with the current casting conditions, oscillating between classic single and double-roll flow patterns. This is likely because pressure sucks the jet up to impinge first on the top surface, or down to impinge on the WF before going towards NF.
- Up-angled nozzles with non-optimal SEN depth could be detrimental in causing both severe surface instability (surface defects) and abnormal downward flow (internal defects) deep into the mold cavity.
- The surface flow instability could increase surface cracks, powder entrapment, and associated downstream problems, especially in advanced high-strength steels.
- Deeper submergence is suggested for up-angled nozzle in this caster system to enable jet flow to impinge first on the NF.
- High-frequency low-amplitude turbulence without surface instability improves mixing, and heat transfer to the meniscus; casting conditions should be chosen to avoid high-power, lower-frequency oscillations.

ACKNOWLEDGEMENTS

The authors thank POSCO and Shin-Eon Kang, POSCO Technical Research Laboratories for providing the water model, and Hyun-Na Bae, Dae-Woo Yoon, and Seung-Ho Shin POSTECH for help with the 1/3 scale water model experiments. Support from the Continuous Casting Consortium, University of Illinois at Urbana-Champaign, POSCO, South Korea (Grant No. 4.0011721.01) and the National Science Foundation (Grant No. 11-30882) is gratefully acknowledged.

REFERENCES

1. T. Teshima, M. Osame, K. Okimoto and Y. Nimura: Poceedings of 71 Steelmaking Conference, The Iron and Steel Society, 1988, pp. 111ima,
2. H. Nakamura, S. Kohira, J. Kubota, T. Kondo, M. Suzuki, and Y. Shiratani: Steelmaking Conference Proceedings, The Iron and Steel Society, 1992, pp. 409-415
3. J. Kubota, K. Okimoto, A. Shirayama, and H. Murakami: Steelmaking Conference Proceedings, The Iron and Steel Society, 1991, pp. 233-241
4. H. L. F. Von Helmholtz: Monatsberichte der Koniglichen, Vol. 23 (1868), pp. 215-228
5. W. Thomson: Philosophical Magazine, Vol. 42 (1871), pp. 362-377
6. T. Funada and D. D. Joseph: J. Fluid, Vol. 445 (2001), pp. 263-283
7. J. Sengupta, B. G. Thomas, H. Shin, G. Lee, and S. Kim: Metall. Mater. Trans. A, Vol. 37A (2006), pp. 1597-1611
8. H. Shin, S. Kim, B. G. Thomas, G. Lee, J. Park, and J. Sengupta: ISIJ Int., Vol. 46 (2006), pp. 1635-1644
9. R. Chaudhary, Go-Gi Lee, B.G. Thomas, and Seon-Hyo Kim: Metall. Mater. Trans. B, Vol. 39B (2008), pp. 870-884
10. Fady M. Najjar, Brian G. Thomas, and Donald E. Hershey: Metall. Mater. Trans. B, Vol. 26B (1995), pp. 749-765
11. Lefeng Zhang, Yufeng Wang and Xiangjun Zuo: Metall. Mater. Trans. B, Vol. 39B (2008), pp.534-550
12. H. Bai and B. G. Thomas: Metall. Mater. Trans. B, Vol. 32B (2001), pp. 253-267